TÜBİTAK

Turkish Journal of Physics

http://journals.tubitak.gov.tr/physics/

Research Article

Turk J Phys
(2015) 39: 81 – 90

doi:10.3906/fiz-1408-4

Studies on mass attenuation coefficient, mass energy absorption coefficient, and kerma for Fe alloys at photon energies of 17.44 to 51.70 keV

Demet YILMAZ*, **Yusuf ŞAHİN, Lütfü DEMİR**
Department of Physics, Faculty of Sciences, Atatürk University, Erzurum, Turkey

Received: 05.08.2014 • **Accepted:** 17.09.2014 • **Published Online:** 23.02.2015 • **Printed:** 20.03.2015

Abstract: The mass attenuation coefficient (μ_m), the mass energy absorption coefficient (μ_{en}/ρ), and kerma relative to air were determined for some alloys, namely $Fe_{0.5}Cr_{0.5}$, $Fe_{0.7}Cr_{0.3}$, $Fe_{0.8}Cr_{0.2}$, $Fe_{0.9}Cr_{0.1}$, $Fe_{0.2}Ni_{0.8}$, $Fe_{0.3}Ni_{0.7}$, $Fe_{0.5}Ni_{0.5}$, $Fe_{0.6}Ni_{0.4}$, $Fe_{0.7}Ni_{0.3}$, and $Fe_{0.8}Ni_{0.2}$, at 17.44, 19.63, 22.10, 24.90, 32.06, 36.39, 37.26, 43.74, 44.48, 50.38, and 51.70 photon energies by using an HPGe detector with a resolution of 182 eV at 5.9 keV. The experimental results of μ_m were compared with the theoretical results. The theoretical values of μ_{en}/ρ were compared with the semiempirical values. It was observed that kerma values relative to air values were different in Fe–Ce and Fe–Ni alloys due to photoelectric cross sections depending on the atomic numbers of the material.

Key words: Mass attenuation coefficient, mass energy absorption coefficient, kerma

1. Introduction

The application of stainless steel alloy in nuclear reactors, modern technology, archeology, and petroleum plants prompts investigation of physical parameters such as the mass attenuation coefficients, the mass energy absorption coefficients, kerma, total atomic and electronic cross-sections, and effective atomic and electron numbers. The mass attenuation coefficient is an essential parameter for gamma ray interactions with the material. The mass attenuation coefficient (μ_m) is a measure of the average number of interactions between incident photons and matter occurring in a given mass-per-unit area thickness of the substance encountered [1].

The mass energy absorption coefficients of materials are important in several applications of medical physics, nuclear science, radiation physics, radiotherapy, irradiation technology, and radiation biology. The absorbed dose in a medium is measured by the mass energy absorption coefficient (μ_{en}/ρ). The photon energy transferred depends on the photon interaction process (photoelectric effect, Compton scattering, and pair production). Thus, μ_{en}/ρ is affected by atomic numbers of material and photon energy. Kerma (kinetic energy released per unit mass) is defined as the initial kinetic energy of all secondary charged particles released per unit mass at a point of interest by uncharged radiation. It is applicable to photons (X-ray, gamma ray, bremsstrahlung, etc.) and neutrons. In the kerma approximation, the effects induced by photons in the chemical content analysis are often scaled in terms of the absorbed dose (collision kerma).

Various researchers have calculated and measured mass attenuation coefficients and mass energy absorption coefficients. Han and Demir investigated mass attenuation coefficients, and effective atomic and electron numbers of Ti and Ni alloys [2]. Saim et al. investigated mass attenuation coefficients, and effective atomic

*Correspondence: ddemir@atauni.edu.tr

and electronic numbers of $Cd_{1-x}Zn_xTe$ alloys in the gamma ray energy region from 10 to 100 keV [3]. The mass attenuation coefficients for 22 high purity elemental materials were measured in the X-ray energy obtained by a variable energy X-ray source range from 13 keV to 50 keV using a high purity germanium detector [4]. Önder et al. obtained mass attenuation coefficients, effective atomic numbers, and electron densities for TLD compounds [5]. Parthasaradhi et al. determined mass attenuation coefficients of tissue equivalent samples in the energy range of 13–44 keV [6]. Manjunathaguru and Umesh determined effective atomic numbers of several biologically important compounds [7]. Akkurt obtained effective atomic numbers for Fe–Mn alloy using a transmission experiment [8].

Hubbell calculated μ_{en}/ρ theoretically for elements and compounds from 1 keV to 20 MeV [9]. Singh et al. investigated energy absorption coefficients for 662 keV gamma rays in some compounds [10]. Seltzer calculated the mass energy-transfer and mass energy absorption coefficients for 1 keV to 100 MeV [11]. The photon energy absorption coefficients of complex molecules such as carbohydrates, proteins, lipids, and vitamins in energy of 200–1500 keV were investigated by Manjunathaguru and Umesh [12]. The energy absorption coefficients in some fatty acids were studied in energy of 662 and 1115 keV by Bhandal et al. [13]. The mass energy absorption coefficients and mass collision stopping powers for electrons in tumors were studied [14]. Shakhreet et al. measured μ_{en}/ρ of paraffin, wax, and gypsum at 662 keV photon energy [15]. Kerma and air kerma are important in radiographic images for image quality. Goçalves et al. investigated the effects of aluminum–copper alloy filtration on photon spectra by air kerma rate [16].

In the present work, mass attenuation coefficients were measured for $Fe_{0.5}Cr_{0.5}$, $Fe_{0.7}Cr_{0.3}$, $Fe_{0.8}Cr_{0.2}$, $Fe_{0.9}Cr_{0.1}$, $Fe_{0.2}Ni_{0.8}$, $Fe_{0.3}Ni_{0.7}$, $Fe_{0.5}Ni_{0.5}$, $Fe_{0.6}Ni_{0.4}$, $Fe_{0.7}Ni_{0.3}$, and $Fe_{0.8}Ni_{0.2}$ alloys at 17.44, 19.63, 22.10, 24.90, 32.06, 36.39, 37.26, 43.74, 44.48, 50.38, and 51.70 photon energies by using an HPGe detector with a resolution of 182 eV at 5.9 keV. The values of μ_{en}/ρ were taken from the compilation of Hubbell and Seltzer [17]. Moreover, the mass energy absorption coefficients were calculated using a semiempirical approximation for the low energy region. The kerma relative to air was computed and reported in the present work.

2. Theoretical background and computational method

The mass attenuation coefficients for materials can be determined by radiation transmission method according to Lambert–Beer's law:

$$I = I_0 \exp\left[-\mu_m t\right], \tag{1}$$

where μ_m is the mass attenuation coefficient (cm^2/g), I_0 is incident photon intensity, I is attenuated photon intensity, and t is the mass thickness of the material. The theoretical μ_m values for the present alloys were obtained by the WinXCom code [18]. This program depends on the use of the mixture rule to calculate the partial and total mass attenuation coefficients for all elements, compounds, and mixtures at standard as well as selected energies.

The mass energy absorption coefficient is the amount of incident photon energy transferred to kinetic energy changed particles by gamma ray interaction [19]. The mass energy absorption coefficient (μ_{en}/ρ) is defined by $\Psi(J\ m^{-2})$. Ψ is the energy fluence of monoenergetic photons passing normally through an area A in an absorber. Moreover, kerma is the energy transferred to charged particles in a volume. Kerma is

$$K = \frac{\Psi A \mu_{en} dx}{\rho A dx} = \Psi\left(\frac{\mu_{en}}{\rho}\right) \tag{2}$$

Therefore, kerma is the product of the energy fluence and the mass energy absorption coefficient. Kerma of an alloy relative to air can be expressed as

$$K_a = \frac{(\mu_{en}/\rho)_{Alloy}}{(\mu_{en}/\rho)_{Air}} = \frac{K_{Alloy}}{K_{Air}} \tag{3}$$

In order to compute kerma relative to air, the values of mass energy absorption coefficients of air and alloys were calculated using the following equation:

$$\frac{\mu_{en}}{\rho} = \sum_i w_i \left(\frac{\mu_{en}}{\rho}\right)_i, \tag{4}$$

where w_i and $(\mu_{en}/\rho)_i$ are the weight fraction and the mass energy absorption coefficient of the ith constituent element present in a material.

3. Experimental details

The experimental setup used in the present study is shown in Figure 1. The source–sample and sample–detector distances were set to 30 mm and 30 mm, respectively. Sharanabasappa et al. suggested the transmission range $0.5 \geq T \geq 0.02$ for HPGe detectors [20]. A variable energy X-ray source from Amersham (AMC.2084) was used in order to irradiate the alloys at energies of 17.44, 19.63, 22.10, 24.90, 32.06, 36.39, 37.26, 43.74, 44.48, 50.38, and 51.70 keV. This source contains a sealed ceramic primary source, ^{241}Am (intensity of 10 mCi), that excites characteristic X-rays from 6 different targets (Cu, Rb, Mo, Ag, Ba, and Tb) in turn (Figure 2). Photon intensities were measured using the HPGe detector. The HPGe detector is a DSG planar high purity germanium crystal with a diameter of 16 mm, a length of 10 mm, a beryllium window of 0.12 mm, and an active area of 200 mm^2. A bias voltage of –1500 V was applied to the detector with a resolution of 182 eV at 5.9 keV.

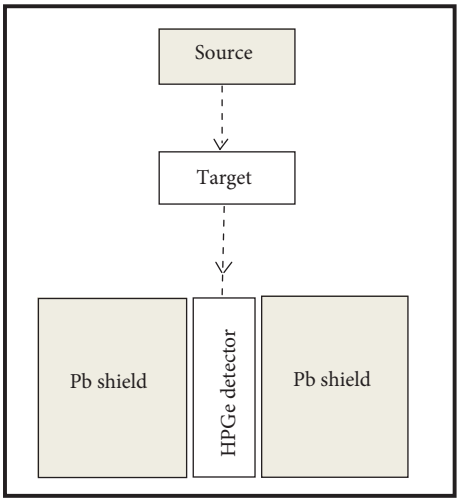

Figure 1. Experimental setup.

The spectra were recorded using by a Canberra (AccuSpec) PC-based multichannel analyzer card. The time constant of the Ortec model 472 amplifier was set to 6 μs, ensuring optimum detector performance as specified by the manufacturer. Operating parameters of the system were governed and controlled by the

computer program Genie-2000. The pulse height spectra of X-rays were acquired for a period of 300–900 s. Background correction was applied to the data collected in 1024 channel of the MCA.

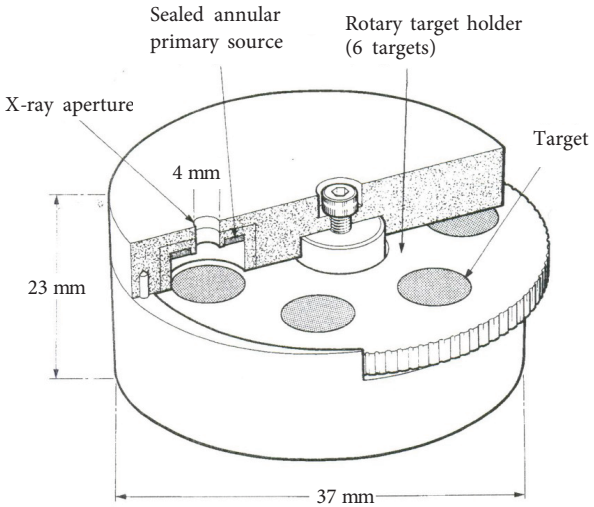

Figure 2. Variable energy X-ray source.

4. Results and discussion

The experimental and theoretical results of the mass attenuation coefficients (μ_m) for various compositions of Fe_xCr_{1-x} and Fe_xNi_{1-x} alloys are tabulated in Table 1. It is evident that the measured values of this parameter were in good agreement with those obtained theoretically. In addition, μ_m depends on the photon energy and the concentration of 3d elements in Fe alloys. There are differences in mass attenuation coefficients for different alloy compositions. The μ_m values for alloys decrease with increasing photon energy. Theoretical calculations performed by WinXCom do not take into account molecular effects, solid-state effects, and interactions between atoms, the photoelectron, and the positively charged ion. This is the reason for the error in the theoretical results. The overall error in the experimental parameters is the sum of the uncertainties in different factors, namely, the evaluation of peak areas (2.12%–4.20%), target mass thickness (1.45%–3.20%), and statistical error ($<$1.00%). Total errors affecting the experimental parameters are 2.76%–5.37%. The errors in the elimination of the background and in the peak fitting procedures are the reason for the error in the experimental results.

The theoretical values of μ_{en}/ρ were calculated by using the mass energy absorption coefficients taken from the compilation of Hubbell and Seltzer [17]. The results are listed in Table 2. Furthermore, the semiempirical approximation was made to μ_{en}/ρ. Manjunathaguru and Umesh have given the simple parameterization of photon mass energy absorption coefficients of samples of biological interest in the high energy region [12]. This empirical formula was used in our previous study [21], but it is not appropriate for composites containing high Z elements and in the low energy region (17.44–51.70 keV). In the low energy region, the mass energy absorption coefficients are related to the mass attenuation coefficients by the following semiempirical relation:

$$\mu_{en}/\rho = (\mu/\rho)\,[0.73509 + (0.17394)/(1 + \exp(\ln E - 3.55427)/0.08471)] \quad (5)$$

The correlation coefficient is 0.998 for this semiempirical formula. The values calculated using the semiempirical expression given are also given in Table 2. It is clear that the present calculated results are in general agreement

Table 1. The mass attenuation coeffcients (μ_m, cm^2/g) for $Fe_x Cr_{1-x}$ and $Fe_x Ni_{1-x}$ alloys.

Alloys										
Energy	$Fe_{0.5}Cr_{0.5}$		$Fe_{0.7}Cr_{0.3}$		$Fe_{0.8}Cr_{0.2}$		$Fe_{0.9}Cr_{0.1}$		$Fe_{0.2}Ni_{0.8}$	
(keV)	Exp.	Theo.	Exp.	Theo.	Exp.	Theo.	Exp.	Theo.	Exp.	Theo.
17.44	33.11 ± 0.91	33.80	34.22 ± 1.33	35.30	35.44 ± 1.13	36.10	34.22 ± 0.99	36.90	44.23 ± 1.59	45.10
19.63	22.34 ± 0.62	24.30	27.33 ± 1.07	25.40	24.21 ± 0.77	25.90	25.34 ± 0.73	26.50	31.49 ± 1.13	32.50
22.10	16.94 ± 0.47	17.40	19.36 ± 0.76	18.20	17.44 ± 0.56	18.60	19.00 ± 0.55	19.00	21.22 ± 0.76	23.40
24.90	11.25 ± 0.31	12.40	12.11 ± 0.47	13.00	12.56 ± 0.40	13.30	12.67 ± 0.37	13.60	16.44 ± 0.59	16.80
32.06	6.45 ± 0.18	6.05	6.89 ± 0.27	6.34	6.21 ± 0.20	6.48	6.23 ± 0.18	6.63	8.77 ± 0.32	8.22
36.39	4.56 ± 0.13	4.23	4.98 ± 0.19	4.43	4.78 ± 0.15	4.53	4.91 ± 0.14	4.63	5.12 ± 0.18	5.75
37.26	3.91 ± 0.11	3.96	4.44 ± 0.17	4.15	4.34 ± 0.14	4.24	4.03 ± 0.12	4.34	5.67 ± 0.20	5.38
43.74	2.34 ± 0.06	2.53	2.78 ± 0.11	2.65	2.77 ± 0.09	2.71	2.95 ± 0.09	2.77	3.09 ± 0.11	3.43
44.48	2.22 ± 0.06	2.41	2.19 ± 0.09	2.53	2.11 ± 0.07	2.59	2.18 ± 0.06	2.64	3.79 ± 0.14	3.28
50.38	1.67 ± 0.05	1.72	1.54 ± 0.06	1.80	1.56 ± 0.05	1.84	1.59 ± 0.05	1.88	2.12 ± 0.08	2.32
51.70	1.63 ± 0.04	1.60	1.22 ± 0.05	1.68	1.16 ± 0.04	1.71	1.33 ± 0.04	1.75	2.19 ± 0.08	2.16

Table 1. Continued.

Alloys										
Energy	$Fe_{0.3}Ni_{0.7}$		$Fe_{0.5}Ni_{0.5}$		$Fe_{0.6}Ni_{0.4}$		$Fe_{0.7}Ni_{0.3}$		$Fe_{0.8}Ni_{0.2}$	
(keV)	Exp.	Theo.	Exp.	Theo.	Exp.	Theo.	Exp.	Theo.	Exp.	Theo.
17.44	45.33 ± 1.99	44.10	43.99 ± 2.16	42.30	43.34 ± 2.32	41.40	41.56 ± 1.29	40.40	40.55 ± 1.18	39.50
19.63	30.35 ± 1.34	31.90	29.66 ± 1.45	30.50	29.55 ± 1.58	29.80	27.89 ± 0.86	29.10	27.79 ± 0.81	28.40
22.10	21.77 ± 0.96	22.90	20.34 ± 1.00	21.90	20.49 ± 1.10	21.40	21.22 ± 0.66	20.90	21.34 ± 0.62	20.40
24.90	17.16 ± 0.76	16.40	16.56 ± 0.81	15.70	14.77 ± 0.79	15.30	13.34 ± 0.41	14.90	13.12 ± 0.38	14.60
32.06	8.23 ± 0.36	8.04	7.94 ± 0.39	7.68	7.67 ± 0.41	7.49	7.56 ± 0.23	7.31	7.45 ± 0.22	7.13
36.39	5.95 ± 0.26	5.62	5.21 ± 0.26	5.37	5.45 ± 0.29	5.24	5.22 ± 0.16	5.11	4.67 ± 0.14	4.99
37.26	5.18 ± 0.23	5.26	5.34 ± 0.26	5.02	4.12 ± 0.22	4.90	4.56 ± 0.14	4.79	4.91 ± 0.14	4.67
43.74	3.99 ± 0.18	3.36	3.78 ± 0.19	3.21	3.67 ± 0.20	3.13	3.77 ± 0.12	3.05	2.11 ± 0.06	2.98
44.48	3.33 ± 0.15	3.20	3.47 ± 0.17	3.06	2.89 ± 0.15	2.99	2.99 ± 0.09	2.92	2.22 ± 0.06	2.84
50.38	2. 98 ± 0.13	2.27	2.98 ± 0.15	2.17	2.38 ± 0.13	2.12	2.22 ± 0.07	2.07	2.55 ± 0.07	2.02
51.70	2.17 ± 0.10	2.12	1.86 ± 0.09	2.02	1.85 ± 0.10	1.98	1.67 ± 0.05	1.93	1.45 ± 0.04	1.88

with the values calculated by the semiempirical expression. It is also clear from Table 2 that the mass energy absorption coefficients depend on the photon energy and chemical content.

Table 2. The mass energy absorption coefficients (μ_{en}/ρ, cm^2/g) for Fe_xCr_{1-x} and Fe_xNi_{1-x} alloys.

Alloys										
Energy	$Fe_{0.5}Cr_{0.5}$		$Fe_{0.7}Cr_{0.3}$		$Fe_{0.8}Cr_{0.2}$		$Fe_{0.9}Cr_{0.1}$		$Fe_{0.2}Ni_{0.8}$	
(keV)	Semiemp.	Theo.	Semiemp.	Theo.	Semiemp.	Theo.	Semiemp.	Theo.	Semiemp.	Theo.
17.44	30.72	30.18	32.09	31.27	32.81	31.81	33.54	32.34	41.00	37.79
19.63	22.08	22.03	23.08	22.86	23.54	23.26	24.08	23.67	29.54	27.72
22.10	15.71	15.93	16.44	16.57	16.80	16.89	17.17	17.20	21.07	20.21
24.90	11.23	11.34	11.78	11.84	12.05	12.09	12.32	12.33	15.22	14.60
32.06	5.22	5.18	5.47	5.48	5.59	5.62	5.72	5.76	7.09	7.15
36.39	3.39	3.41	3.55	3.62	3.63	3.72	3.71	3.82	4.61	4.95
37.26	3.13	3.15	3.28	3.35	3.35	3.44	3.43	3.54	4.25	4.62
43.74	1.89	1.87	1.98	1.99	2.02	2.04	2.07	2.10	2.56	2.89
44.48	1.79	1.78	1.88	1.89	1.93	1.94	1.97	1.99	2.44	2.75
50.38	1.27	1.27	1.33	1.32	1.36	1.35	1.39	1.38	1.71	1.92
51.70	1.18	1.19	1.24	1.25	1.26	1.27	1.29	1.30	1.59	1.78

Table 2. Continued.

Alloys										
Energy	$Fe_{0.3}Ni_{0.7}$		$Fe_{0.5}Ni_{0.5}$		$Fe_{0.6}Ni_{0.4}$		$Fe_{0.7}Ni_{0.3}$		$Fe_{0.8}Ni_{0.2}$	
(keV)	Semiemp.	Theo.	Semiemp.	Theo.	Semiemp.	Theo.	Semiemp.	Theo.	Semiemp.	Theo.
17.44	40.09	37.20	38.45	35.99	37.63	35.38	36.72	34.76	35.90	34.13
19.63	28.99	27.28	27.72	26.38	27.08	25.93	26.45	25.47	25.81	25.00
22.10	20.62	19.88	19.71	19.22	19.26	18.88	18.80	18.54	18.35	18.20
24.90	14.86	14.35	14.22	13.86	13.86	13.60	13.50	13.35	13.23	13.09
32.06	6.94	7.00	6.63	6.69	6.46	6.54	6.31	6.38	6.15	6.22
36.39	4.51	4.83	4.31	4.57	4.20	4.45	4.10	4.32	4.00	4.19
37.26	4.16	4.50	3.97	4.26	3.88	4.13	3.79	4.01	3.69	3.89
43.74	2.51	2.80	2.40	2.62	2.34	2.53	2.28	2.43	2.22	2.34
44.48	2.38	2.67	2.28	2.49	2.23	2.40	2.17	2.31	2.11	2.22
50.38	1.67	1.86	1.60	1.73	1.56	1.67	1.53	1.60	1.49	1.54
51.70	1.56	1.72	1.49	1.61	1.46	1.55	1.42	1.50	1.39	1.44

The energy dependence of kerma relative to air is shown in Table 3. It is clearly seen that kerma depends on the chemical content. However, there is a large variation in kerma for Fe alloys containing Cr and Ni. Kerma values for Fe_xCr_{1-x} and Fe_xNi_{1-x} alloys increase with increasing photon energy until 32.06 and 36.39 keV, respectively. Later, kerma values decrease with increasing photon energy. The reason for such variation in kerma is the photoelectric cross section proportional to Z^{4-5}.

The contribution of coherent (Rayleigh) scattering, incoherent (Compton) scattering, and the photoelectric process to total photon interaction can be verified using XCOM software for some alloys. As seen from Table 4, Compton scattering contributes about 6.35% to total interaction at 51.70 keV, whereas coherent scattering contributes only 6.11% and the photoelectric process about 87.54% for $Fe_{0.2}Ni_{0.8}$. The contributions to total photon interaction depend on the concentration of 3d metals as seen from Table 4.

Table 3. Calculated values of kerma relative to air.

Alloys										
Energ (keV)	$Fe_{0.5}Cr_{0.5}$	$Fe_{0.7}Cr_{0.3}$	$Fe_{0.8}Cr_{0.2}$	$Fe_{0.9}Cr_{0.1}$	$Fe_{0.2}Ni_{0.8}$	$Fe_{0.3}Ni_{0.7}$	$Fe_{0▷5}Ni_{0▷5}$	$Fe_{0▷6}Ni_{0▷4}$	$Fe_{0▷7}Ni_{0▷3}$	$Fe_{0▷8}Ni_{0▷2}$
17.44	35.89	37.19	37.83	38.46	44.94	44.24	42.80	42.08	41.34	40.59
19.63	37.98	39.42	40.11	40.81	47.80	47.04	45.48	44.71	43.92	43.11
22.10	40.51	42.14	42.95	43.74	51.39	50.55	48.87	48.01	47.15	46.28
24.90	43.48	45.40	46.36	47.28	55.98	55.02	53.14	52.15	51.19	50.19
32.06	48.48	51.29	52.60	53.91	66.92	65.52	62.62	61.21	59.71	58.22
36.39	47.36	50.28	51.67	53.06	68.76	67.09	63.48	61.81	60.00	58.20
37.26	46.66	49.62	50.95	52.44	68.43	66.66	63.10	61.18	59.40	57.62
43.74	38.67	41.15	42.18	43.42	59.76	57.90	54.18	52.32	50.25	48.39
44.48	37.71	40.04	41.10	42.16	58.26	56.57	52.75	50.85	48.94	47.03
50.38	30.50	31.70	32.42	33.15	46.11	44.67	41.55	40.11	38.43	36.99
51.70	29.05	30.51	31.00	31.73	43.45	41.98	39.30	37.83	36.61	35.15

Table 4. The contributions verified using XCOM to total photon interaction for some alloys (%).

Energy	$Fe_{0.2}Ni_{0.8}$			$Fe_{0.8}Ni_{0.2}$			$Fe_{0.3}Ni_{0.7}$			$Fe_{0.7}Ni_{0.3}$		
(keV)	Coh.	Comp.	Photo.	Coh.	Comp.	Photo.	Coh.	Comp.	Photo.	Coh.	Comp.	Photo.
17.44	1.54	0.25	98.22	1.61	0.28	98.11	1.55	0.25	98.20	1.60	0.27	98.13
19.63	1.83	0.36	97.82	1.92	0.41	97.67	1.84	0.36	97.80	1.91	0.40	97.70
22.10	2.16	0.51	97.33	2.28	0.59	97.14	2.17	0.52	97.30	2.25	0.57	97.17
24.90	2.54	0.74	96.72	2.67	0.85	96.48	2.55	0.75	96.69	2.65	0.83	96.51
32.06	3.52	1.60	94.88	3.71	1.82	94.46	3.55	1.63	94.82	3.67	1.79	94.54
36.39	4.10	2.33	93.57	4.33	2.67	93.00	4.15	2.39	93.47	4.28	2.60	93.11
37.26	4.22	2.49	93.29	4.45	2.85	92.70	4.26	2.55	93.19	4.41	2.78	92.81
43.74	5.10	3.96	90.94	5.38	4.54	90.08	5.12	4.05	90.83	5.33	4.41	90.26
44.48	5.19	4.15	90.66	5.49	4.75	89.76	5.24	4.24	90.51	5.42	4.63	89.94
50.38	5.94	5.89	88.17	6.28	6.72	87.00	5.98	6.03	87.99	6.25	6.59	87.17
51.70	6.11	6.35	87.54	6.45	7.25	86.31	6.19	6.47	87.35	6.38	7.05	86.57

5. Conclusions

This experimental study was undertaken to obtain information on $\mu_m, \mu_{en}/\rho$ and kerma for Fe_xCr_{1-x} and Fe_xNi_{1-x} alloys. The results show that μ_m is a useful and sensitive physical quantity to determine the μ_{en}/ρ for alloys. Values of $\mu_m, \mu_{en}/\rho$ and kerma depend on the photon energy and chemical content of the investigated alloys. The photon interaction parameters should also be investigated to confirm the applicability of the mixture rule at different energies. $\mu_m, \mu_{en}/\rho$ and kerma at high energies must be investigated since Fe_xCr_{1-x} and Fe_xNi_{1-x} alloys have large-scale usage in the technology of stainless steel production, nuclear science, and geosciences.

References

[1] Jackson, D. F.; Hawkes, D. J. *Phys. Rep.* **1981**, *70*, 169–233.

[2] Angelonea, M.; Bubbab, T.; Espositoc, A. *Appl. Radiat. Isot.* **2001**, *55*, 505–511.

[3] Önder, P.; Tursucu, A.; Demir, D.; Gürol, A. *Nucl. Instrum. Methods B* **2012**, *292*, 1–10.

[4] Parthasaradhi, K.; Esposito, A.; Pelliccioni, M. *Int. J. Appl. Radiat. Isot. A* **1992**, *43*, 1481–1486.

[5] Manjunathaguru, V.; Umesh, T. K. *J. Phys. B. At. Mol. Opt. Phys.* **2006**, *39*, 3969–3981.

[6] Akkurt, I. *Chin. Phys. Lett.* **2007**, *24*, 2812–2814.

[7] Hubbbell, J. H. *Int. J. Appl. Radiat. Isot.* **1982**, *33*, 1269–1290.

[8] Singh, K.; Rani, R.; Kumar, V.; Deep, K. *Appl. Radiat. Isot.* **1996**, *47*, 697–698.

[9] Seltzer, S. M. *Radiation Research* **1993**, *136*, 147–170.

[10] Manjunathaguru, V.; Umesh, T. K. *Pramana Journal of Sciences* **2009**, *72*, 375–387.

[11] Bhandal, G. S.; Singh, K.; Rani, R.; Kumar, V. *Appl. Radiat. Isot.* **1994**, *45*, 379–381.

[12] Maughan, R. L.; Chuba, P.; Porter, E.; Ben-Josef, A. T.; Lucas, D. R.; Bjarngard, B. E. *Medical Physics* **1999**, *26*, 472–477.

[13] Shakhreet, B. Z.; Chong, C. S.; Bandyopadhyay, T.; Bradley, D. A.; Tajuddin, A. A.; Shukri, A. *Rad. Phys. Chem.* **2003**, *68*, 757–764.

[14] Gonçalves, A.; Rollo, J. M. D. A.; Gonçalves, M.; Neto, F. H.; Bóscolo, F. N.; *Braz. Dent. J.* **2004**, *15*, 214–219.

[15] Hubbell, J. H.; Seltzer, S.M. **1995** *NISTIR*-5632.

[16] Gerward, L.; Guilbert, N.; Jensen, K. B.; Levring, H. *Radiat. Phys. Chem.* **2001**, *60*, 23–24.

[17] International Commission on Radiation Units and Measurements, Report 33, 7910 Woodmont Avenue Washington, D. C. 2014, USA.

[18] Sharanabasappa; Kerur, B. R.; Anilkumar, S.; Hanumaiah, B. *Appl. Radiat. Isot.* **2010**, *68*, 76–83.

[19] Demir, D.; Turşucu, A. *Annals of Nuclear Energy* **2012**, *48*, 17–20.